Kinetic studies on the CO oxidation on Pd(111) with low energy electron diffraction (LEED) and angle-resolved thermal desorption

Tatsuo Matsushima and Hiromu Asada
Research Institute for Catalysis, Hokkaido University, Sapporo 060, Japan

(Received 4 February 1986; accepted 22 April 1986)

Three different coadsorption structures of CO and oxygen over Pd(111) were analyzed through measurements of the intensity of LEED spots; separate domains of $p(2\times2)$–O and $(\sqrt{3}\times\sqrt{3})R\ 30°$–CO, closely contacted domains of $(\sqrt{3}\times\sqrt{3})R\ 30°$–O with the same structure of CO, and also a mixed phase with (2×1) periodicity. The desorption of CO_2 produced in the above adlayers was analyzed in an angle-resolved form. The angular distribution becomes extremely sharp, when the reaction sites are closely surrounded by coadsorbates. The collimation of the desorption along the surface normal is suggested to be due to the collision of desorbing CO_2 with the surrounding adsorbates, as well as the repulsive interaction between nascent CO_2 and the surface.

I. INTRODUCTION

The oxidation of carbon monoxide over platinum metals is a suitable model reaction for the analysis of the energy distribution among the internal and translational degrees of freedom in the product molecule.[1] The product CO_2 interacts only weakly with the surface.[2–4] Once CO_2 is formed it will immediately be released into the gas phase. In such a case, the translational energy (or the angular distribution) may be controlled by the interaction between the surface and the whole product molecule at the instant of formation.[5–8] It frequently has an excess energy compared with the surface temperature.[9,10] The mutual interaction of the reactants, CO(a)$\longleftrightarrow$O(a), will affect the energy distribution in the internal modes.[11,12] This interaction contributes largely to the activation energy for the CO_2 formation.

This consideration leads to the idea that the angular distribution may be affected by the local configuration of adsorbates around the reaction site. Our recent work on Rh(111) supports this idea; the angular distribution becomes sharp when the CO_2 formation site is closely surrounded.[7] The relation between the angular distribution and the local configuration around reaction sites will be examined more suitably on Pd(111). Because the coadsorption of CO and oxygen on this surface produces different structures depending on the coverages[13]; CO(a) and O(a) are randomly distributed for small coverages. The adspecies form separate domains of $p(2\times2)$–O and $(\sqrt{3}\times\sqrt{3})R\ 30°$–CO when the coverages increase. Further admission of CO causes a compression of $p(2\times2)$–O into $(\sqrt{3}\times\sqrt{3})R\ 30°$. The latter is further compressed locally to a structure with (2×1) periodicity. These coadsorption structures may yield sites for the formation of CO_2 which would show different angular distributions.

In this paper the above prediction will be confirmed. First, we report the quantitative analysis of the above adsorption structures. It supports the previous work by Conrad *et al.*[13] Second, the formation of CO_2 observed at different temperatures during thermal desorption is assigned to the reaction sites in the above coadlayers. Third, the angular distribution of the desorption of CO_2 will be analyzed by angle-resolved thermal desorption. This method is useful in the present low temperature experiments.[3] Finally several factors which contribute to the angular distribution will be discussed.

II. EXPERIMENTAL

The experimental apparatus and procedures were essentially the same as those reported previously.[3] The apparatus consisted of a reaction chamber (with LEED-AES), an analyzer chamber, and a collimator placed between them.

The single crystal sample was a disk-shaped slice (10 mm diameter$\times$0.8 mm thickness, purity 99.995% from Metal Crystal Ltd., U.K.). Both faces were polished with standard metallographic techniques. The sample was set on a rotatable axis perpendicular to the axis of the collimator. It was cleaned by prolonged Ar^+ bombardment in the range from room temperature to 800 K, and heating in oxygen of 1×10^{-8} Torr at 800 K. After the crystal was flashed *in vacuo* up to 1100 K, no impurity was detected with AES. The LEED pattern displayed a sharp (1×1) structure at this stage. The crystal was annealed to 1100 K before each experimental run.

The spot intensity of LEED patterns was followed with a spot photometer of a photomultiplier tube. The signal was recorded when the heater current to control the surface temperature was momentarily off. In thermal desorption experiments the sample covered by oxygen and/or CO was resistively heated, while the amount of CO_2 passing through the collimator was monitored with a mass spectrometer in the analyzer chamber (angle-resolved spectra). Desorption spectra were also recorded in an angle-integrated form with another mass spectrometer in the reaction chamber. The latter was used to determine the coverage of CO and oxygen, and also to analyze the general kinetic features of the CO_2 formation. The signal in the angle-integrated form involves the contribution from the side of the sample ($\sim$14% of the total area).

 0021-9606/86/151658-11$02.10

III. RESULTS

A. Adsorption of CO and oxygen

The relative coverage of CO and oxygen was determined with thermal desorption. The desorption of CO showed a single peak around 500 K. The peak area increased linearly up to 1.7 L (langmuir) with the increasing exposure. Below the absolute coverage (the ratio of CO admolecules to surface Pd atoms) of $\theta_{CO} = 1/2$, the adsorption rate was independent of the surface temperature in the range of 100–300 K. The LEED spot intensity of $(\sqrt{3}\times\sqrt{3})R\,30°$–CO in the course of the exposure, which was measured at 190 K or below, showed a maximum at 1.1 L. This dosage, $Q_{CO,\sqrt{3}}$, was concluded to be required for the completion of the structure, i.e., $\theta_{CO} = 1/3$. It indicates that the sticking coefficient is close to unity.[14] Below 150 K, the maximum spot intensity was observed at the same exposure after the surface covered by CO was annealed up to 300 K and cooled again to the adsorption temperature. The intensity increased fairly linearly with the coverage below $\theta_{CO} = 1/3$. It suggests that CO forms domains of $(\sqrt{3}\times\sqrt{3})R\,30°$ from small coverages.

Oxygen dissociates easily above 220 K[15] and forms a $p(2\times2)$ lattice.[13] The LEED spot intensity increased monotonously with the exposure. The thermal desorption showed a single peak in the range of 750–850 K when the adsorption temperature was above 220 K. The peak area increased monotonously with the exposure. The relative coverage of oxygen adatoms $\theta_O/\theta_{O,max}$ is represented as the peak area relative to the maximum area at large exposures (>20 L). The maximum area corresponds to a quarter of the monolayer. The initial sticking coefficient was estimated to be 0.43, which agreed with the literature value.[14] It remained almost constant below $\theta_O/\theta_{O,max}$, $= 0.3$. Above this coverage it decreased fairly linearly with the increasing coverage.

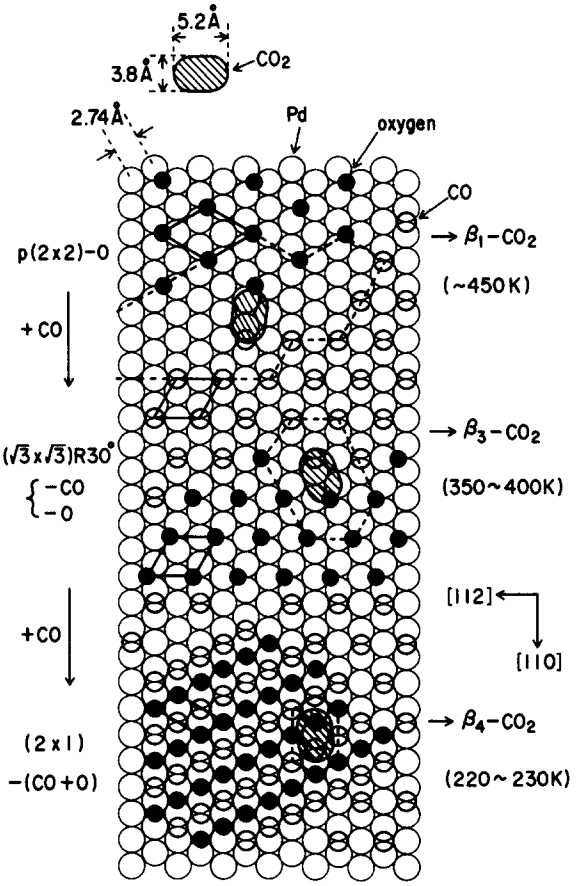

FIG. 1. Sketch of the structural transformations which take place when an oxygen covered surface is exposed to CO. $p(2\times2)$–O domains coexist with $(\sqrt{3}\times\sqrt{3})R\,30°$–CO domains. The former are compressed into $(\sqrt{3}\times\sqrt{3})R\,30°$–O with the increasing CO exposure. Further CO admission induces regions of a mixed (O + CO) structure with (2×1) periodicity. Dashed lines indicate free spaces around reaction sites. Ellipses represent the size of a CO_2 molecule estimated from van der Waals' radii.

B. Coadsorption of oxygen and CO

Our LEED data confirm the structure analysis by Conrad *et al.*,[13] i.e., admission of CO causes a compression of $p(2\times2)$–O into $(\sqrt{3}\times\sqrt{3})R\,30°$. Further dosage of CO leads to the formation of regions with (2×1) periodicity. The structure proposed is schematically drawn in Fig. 1. They have not quantitatively analyzed the structure through mea-

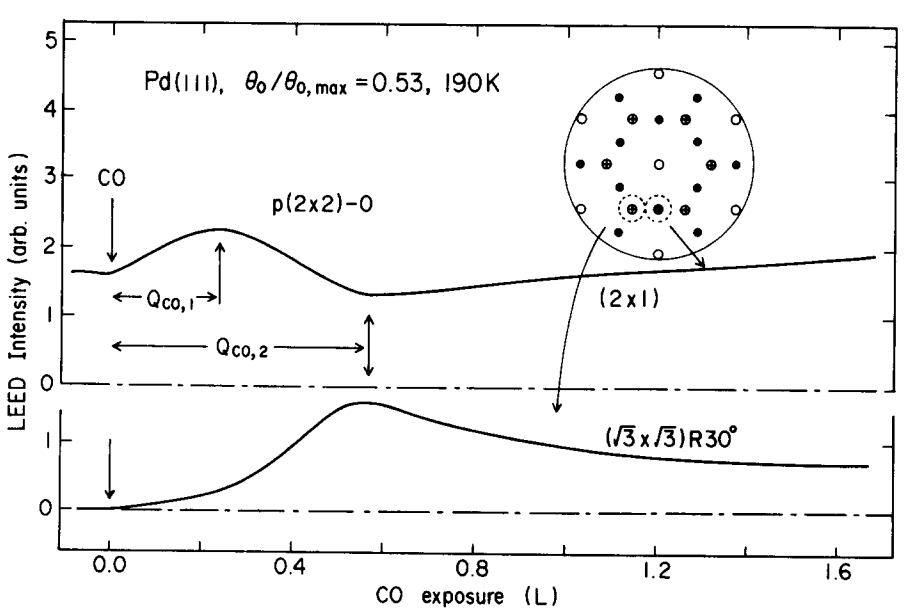

FIG. 2. Variation of LEED spot intensity due to (2×2) and $(\sqrt{3}\times\sqrt{3})R\,30°$ structures. The surface covered by oxygen at 300 K was exposed to CO at 2.5×10^{-9} Torr at the 190 K. The inserted figure represents a LEED pattern; O: substrate spot, ●: (2×2), ⊕: $(\sqrt{3}\times\sqrt{3})R\,30°$. Dotted circles around spots indicate the area accepted by the spot photometer. The beam voltage was 59 eV for (2×2) and 64 eV for $(\sqrt{3}\times\sqrt{3})R\,30°$.

surements of the spot intensity in the course of the above compression.

We followed the spot intensity of $p(2\times2)$ and $(\sqrt{3}\times\sqrt{3})R$ 30° at temperatures of 100–400 K. The above compression was well observed at 190 K, where the oxidation occurred very slowly even at high reactant exposures. Typical variations of the spot intensity were reproduced in Fig. 2. The surface was first exposed to O_2 at 300 K to the extent of $\theta_O/\theta_{O,max} = 0.53$. After the surface temperature was maintained at 190 K, CO was introduced at 2.5×10^{-9} Torr. The acceptance angle of the spot photometer was fixed at 2°. The meter accepted the photointensity from the area indicated by dotted circles in the LEED pattern inserted in the figure. No background intensity was subtracted.

The intensity of $p(2\times2)$–O was increased by a small CO exposure. With further admission of CO it showed a maximum at 0.23 L and a minimum at 0.56 L. On the other hand, the intensity due to $(\sqrt{3}\times\sqrt{3})R$ 30° began to increase rapidly around the maximum of $p(2\times2)$–O. It showed a maximum at the same exposure as the minimum of $p(2\times2)$–O. Above this exposure the surface showed regions with (2×1) periodicity beside CO domains with $\theta_{CO} > 1/3$. The first increase of the (2×2)–O intensity indicates that oxygen domains become larger. CO molecules which adsorb near oxygen adatoms may repel the latter into their domains, since the interaction between CO(a) and O(a) is repulsive.[13] At the maximum intensity of $p(2\times2)$–O the surface holds the maximum amount of CO which can be adsorbed without causing the compression of the oxygen lattice. This exposure is designated as $Q_{CO,1}$. The other interesting exposure $Q_{CO,2}$ represents the CO exposure required for maximizing the intensity of $(\sqrt{3}\times\sqrt{3})R$ 30° structure. It indicates the exposure for completion of the transformation from $p(2\times2)$–O into $(\sqrt{3}\times\sqrt{3})R$ 30°.

Both quantities are functions of the initial coverage of oxygen. $Q_{CO,1}$ increased linearly with the increasing area unoccupied by oxygen $(1-\theta_O/\theta_{O,max})$ as shown in Fig. 3. The ordinate was normalized by $Q_{CO,\sqrt{3}}$ (= 1.1 L), the CO exposure required for completion of $(\sqrt{3}\times\sqrt{3})R$ 30°–CO on a clean surface. The solid line, having a slope of unity, shows the relation which would be observed if the unoccupied area were covered completely with CO domains of $(\sqrt{3}\times\sqrt{3})R$ 30° without compression of the oxygen lattice. Experimental results show that the quantity of $Q_{CO,1}/Q_{CO,\sqrt{3}}$ falls far below the solid line. It attained almost halfway up to the line. This means that there is a considerable free space between $p(2\times2)$–O domains and CO domains. The latter forms probably $(\sqrt{3}\times\sqrt{3})R$ 30° domains, since CO can form this structure below $\theta_{CO} = 1/3$ and the repulsive interaction with O(a) can accelerate the formation.

The compression of the oxygen lattice into the $(\sqrt{3}\times\sqrt{3})R$ 30° structure is complete at $Q_{CO,2}$. At this stage the $(\sqrt{3}\times\sqrt{3})R$ 30° spot intensity must be contributed from both oxygen and CO domains. The minimum of (2×2)–O always appeared at the same exposure as the maximum of $(\sqrt{3}\times\sqrt{3})R$ 30°. This agreement suggests that both domains have almost complete $(\sqrt{3}\times\sqrt{3})R$ 30° structure at $Q_{CO,2}$. Above this exposure, both domains begin to be compressed into structures more dense than the local coverage of 1/3. Beyond the intensity minimum of the (2×2) spot, these half-order spots should be due to the contribution of domains with (2×1) periodicity. In order to examine the density of the CO domains the amount of $Q_{CO,2}$ was compared with $Q_{CO,\sqrt{3}}(1-3\theta_O/4\theta_{O,max})$ in Fig. 4. The latter indicates the CO exposure required for completion of $(\sqrt{3}\times\sqrt{3})R$ 30°–CO domains outside oxygen domains with the same structure. In this consideration, the sticking coefficient is assumed to be invariant since oxygen adatoms do not prevent CO from adsorbing.[13] The solid line represents this ideal case. Experimental data shown by squares fit this model. No free space is expected between both domains.

The dependence of $Q_{CO,1}$ and $Q_{CO,2}$ upon the surface temperature and the CO pressure was studied, in order to

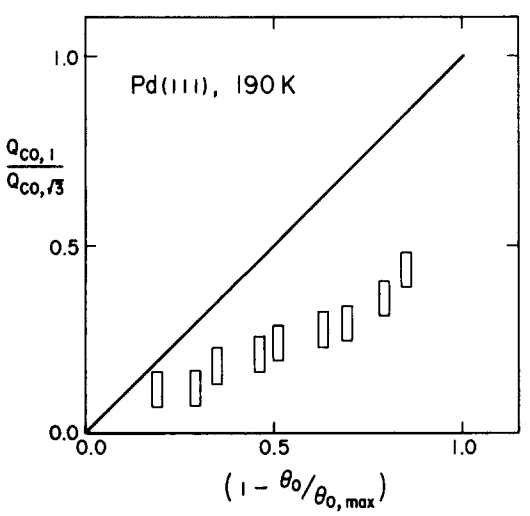

FIG. 3. Dependence of the CO exposure for maximizing the $p(2\times2)$–O intensity on area unoccupied with oxygen. The solid line indicates an ideal case (see the text).

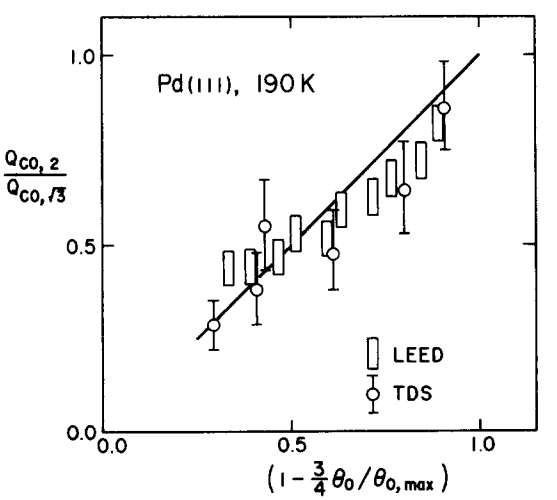

FIG. 4. Variation of the CO exposure for completion of the transformation from $p(2\times2)$ into $(\sqrt{3}\times\sqrt{3})R$ 30° structure with surface area unoccupied by oxygen. The solid line represents an ideal case (see the text).

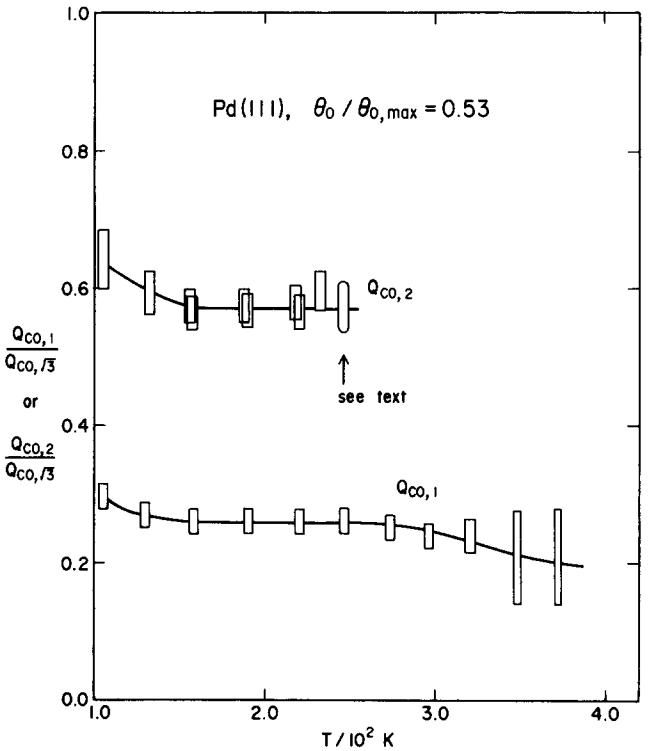

FIG. 5. Values of $Q_{CO,1}$ and $Q_{CO,2}$ determined at various surface temperatures. The surface was first covered by oxygen at 300 K. It was exposed to CO (2.5×10^{-9} Torr) at desired temperatures.

examine whether the diffusion of the adspecies is rapid as compared with CO adsorption. The results are summarized in Figs. 5 and 6. The value of $Q_{CO,1}$ was constant in the temperature range of 130–300 K. Above 300 K, the maximum of the intensity due to $p(2\times2)$–O became unclear, inasmuch as the reaction occurred. $Q_{CO,2}$ showed a constant value in the range of 130–230 K. Above this range, no maximum of the intensity due to $(\sqrt{3}\times\sqrt{3})R$ 30° was observed. Because a new reaction pathway (β_4–CO_2 formation) is opened, as shown below. At 240 K, the intensity increased monotonously with the increasing CO exposure. The ellipse in the figure indicates the CO exposure at which the intensity

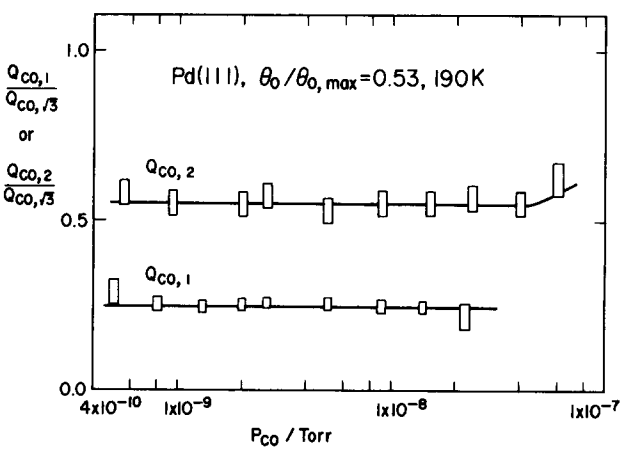

FIG. 6. Values of $Q_{CO,1}$ and $Q_{CO,2}$ determined at various CO pressures. The surface covered by oxygen was exposed to CO at 190 K.

reached an almost constant value. Below 130 K, the two intensity maxima became unclear, and further, the increments of the intensity were not significant. Probably the diffusion of O(a) and also CO(a) is not fast.

The values of $Q_{CO,1}$ and $Q_{CO,2}$ determined at 190 K were independent of the exposure pressure of CO in the range of 5×10^{-10}–2×10^{-8} Torr. It can be concluded that the diffusion of the adspecies is fast enough to construct equilibrium coadsorption structures under the conditions used here.

Now we find three different sites for the interaction of CO with oxygen, i.e., between $p(2\times2)$–O domains and $(\sqrt{3}\times\sqrt{3})R$ 30°–CO domains, between CO and oxygen domains of $(\sqrt{3}\times\sqrt{3})R$ 30°, and also in high density domains with (2×1) periodicity. The structure of (2×1) domains has been proposed,[13] where CO and oxygen adatoms have close contact, as shown in Fig. 1. No new information was added to this proposal in our experiments. In the next section, spectra of CO_2 produced by heating the above coadsorption layers will be summarized. The peak temperature of CO_2 is characteristic of the local configuration of the adsorbates around the reaction sites.

C. Sites for CO_2 formation

CO_2 formation spectra depended strongly on the amounts of CO and oxygen exposure, adsorption temperature, and the exposure sequence. When the surface was first exposed to O_2 and then to CO, two CO_2 peaks were observed. The CO_2 spectra, however, showed a single peak when CO was first dosed. Such behavior has already been reported.[13] The adsorption temperature used in the previous studies[13] was 240 K in most cases, where the oxidation occured considerably during the preparation of coadlayers. We prepared the coadsorption layers at temperatures of 100–400 K. No essential difference was found in the CO_2 spectra, when the surface covered by oxygen was exposed to CO below 200 K. Above this temperature, CO_2 is significantly formed during CO exposure (before thermal desorption procedures), especially at high CO exposures.

Typical CO_2 formation spectra were reproduced in Fig. 7. The procedures to prepare coadlayers were the same as those used in Fig. 2. At a desired exposure of CO, the gas supply was terminated and the surface was heated with a constant voltage up to 1100 K. The temperature increased linearly with a rate of 20 K/s below 500 K. The resultant CO_2 spectra will be compared with the spot intensity variations shown in Fig. 2. Only a single peak of CO_2 was observed around 450 K, when the surface was covered by separate domains of $(\sqrt{3}\times\sqrt{3})R$ 30°–CO and $p(2\times2)$–O, i.e., at CO exposures below $Q_{CO,1}$. This CO_2 is produced between separate domains, where large free spaces exist. Such CO_2 is called β_1-CO_2 over Rh(111).[7] At exposures between $Q_{CO,1}$ ($=0.23$ L) and $Q_{CO,2}$ ($=0.56$ L), the CO_2 peak became broad and was shifted to 410 K with the increasing CO exposure. This CO_2 involves β_1-CO_2 and also β_3-CO_2. The latter is produced between domains of $(\sqrt{3}\times\sqrt{3})R$ 30° of oxygen and CO. The peak of β_3-CO_2 was shifted to 350 K with the increasing CO exposure. Around 0.7 L CO, a new peak (β_4-

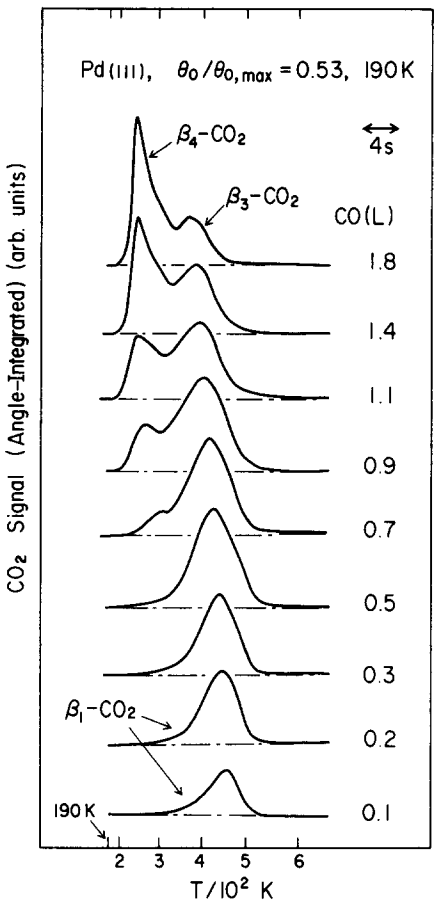

FIG. 7. Variation of CO_2 spectra with CO exposures. The surface partially covered by oxygen was exposed to CO at 190 K. The heating rate was ~20 K/s.

CO_2) appeared. The onset of β_4-CO_2 formation was estimated to be 0.6 L CO from the variation of the peak height with CO exposures. This position depended on the initial oxygen coverage. They were plotted as vertical bars in Fig. 4. They agreed well with the onset of the compression of $(\sqrt{3}\times\sqrt{3})R$ 30°. β_4-CO_2 can be concluded to be produced in the highly compressed (2×1) structure. The above assignment of the reaction sites for CO_2 agrees generally with the previous studies.[13]

During thermal desorption the coverage of CO and oxygen decreases through the removal as CO_2. Therefore, the coadsorption structure will change during heating procedures. LEED patterns were observed after the coadlayer prepared at 190 K was annealed slowly (~2 K/s) to a desired temperature, T_p, and cooled again to 190 K. Typical results at $\theta_O/\theta_{O,max} = 0.53$ are summarized in Table I. The $(\sqrt{3}\times\sqrt{3})R$ 30° lattice below 0.5 L CO was relaxed to the (2×2) lattice during thermal desorption. In thermal desorption procedures both β_1 and β_3-CO_2 may be produced. Above 0.9 L CO, the (2×1) lattice was relaxed to the $(\sqrt{3}\times\sqrt{3})R$ 30° lattice above $T_p = 250$ K. In this case the thermal desorption is expected to show the formation of β_4-CO_2 at low temperatures and that of β_3-CO_2 at high temperatures, as actually observed.

However, when the initial oxygen coverage was relatively small and the CO exposure was very high (see Fig. 8), only β_4-CO_2 was observed. The CO coverage remained essentially constant during CO_2 formation and the (2×1) structure was kept compressed to the depletion of oxygen.

Figure 1 summarizes these reaction sites. There is a considerable free space around the site for β_1-CO_2 formation. The sites for β_3-CO_2 formation are fairly surrounded by the fringes of CO and oxygen domains. Dashed lines indicate the surrounding adspecies around the reaction sites. The sites for β_4-CO_2 are closely surrounded by CO and oxygen adatoms.

D. Kinetic studies

The CO_2 formation showed no essential change in the spectra even when the surface precovered by oxygen was exposed to CO at 100 K. It is suggested that the diffusion of adspecies becomes fast during heating procedures and the equilibrium coadsorption structures are formed. As shown below, CO_2 is produced slowly even below 190 K. Therefore the kinetic studies described below are based on CO_2 spectra generated from coadlayers prepared at 100 K, where the reaction can be stopped completely.

The desorption of CO_2 produced in the reaction sites described above shows different angular distributions. We will compare first the peak height ratio of β_4-CO_2 to β_3-CO_2 or β_1-CO_2 in the angle-integrated form with a similar ratio observed at the normal direction in the angle-resolved form.

TABLE I. LEED patterns observed when the surface covered by oxygen and CO was heated. The surface was first covered by oxygen ($\theta_O/\theta_{O,max} = 0.53$) at 300 K and further exposed to CO at 190 K. It was heated sequentially up to 450 K. LEED patterns were observed at 190 K.[a] The maximum intensity of the spots was compared in the range of 59–65 eV of the beam energy.

CO(L)	Annealing temperature T_p (K)					
	190	250	310	350	400	450
0.20	s(2)	s(2)	s(2)>($\sqrt{3}$)	s(2)>($\sqrt{3}$)	f($\sqrt{3}$)	...
0.50	(2)<($\sqrt{3}$)	(2)<($\sqrt{3}$)	(2)>($\sqrt{3}$)	(2)>($\sqrt{3}$)	...	...
0.90	(2)>($\sqrt{3}$)	(2)≪($\sqrt{3}$)	s($\sqrt{3}$)	($\sqrt{3}$)	b($\sqrt{3}$)	...
1.4	s(2)>($\sqrt{3}$)	sp($\sqrt{3}$)	sp($\sqrt{3}$)	($\sqrt{3}$)	b($\sqrt{3}$)	...
1.8	s(2)	sp($\sqrt{3}$)	sp($\sqrt{3}$)	($\sqrt{3}$)	b($\sqrt{3}$)	...

[a] LEED pattern; (2) = $p(2\times2)$ or (2×1), ($\sqrt{3}$) = $(\sqrt{3}\times\sqrt{3})R$ 30°. Diffraction spot; <: more intense, ≪: much more intense, s: sharp, f: faint, b: broad and sp: split.

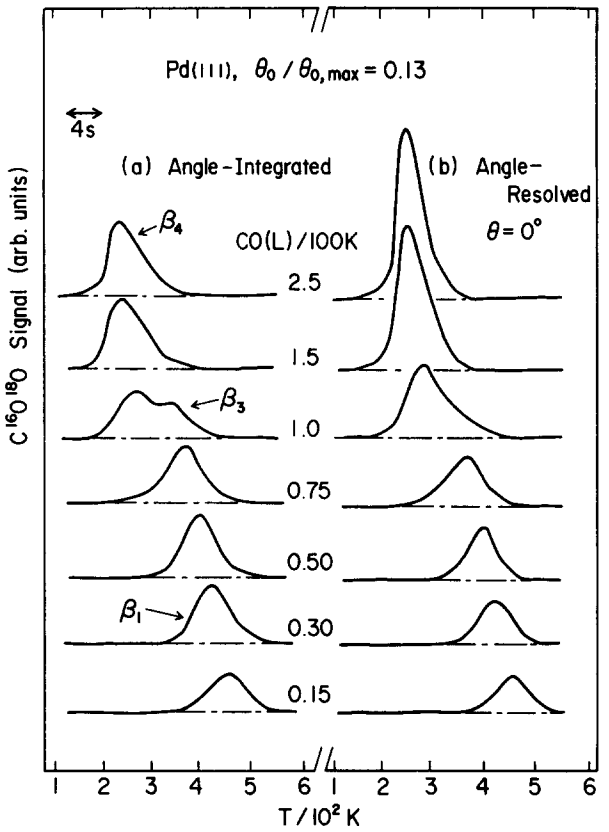

FIG. 8. Variation of CO_2 spectra generated at a small oxygen coverage in angle-integrated (a) the angle-resolved (b) forms with various CO exposures. The surface covered with oxygen was exposed to CO in various amounts at 100 K. The heating rate was ~20 K/s.

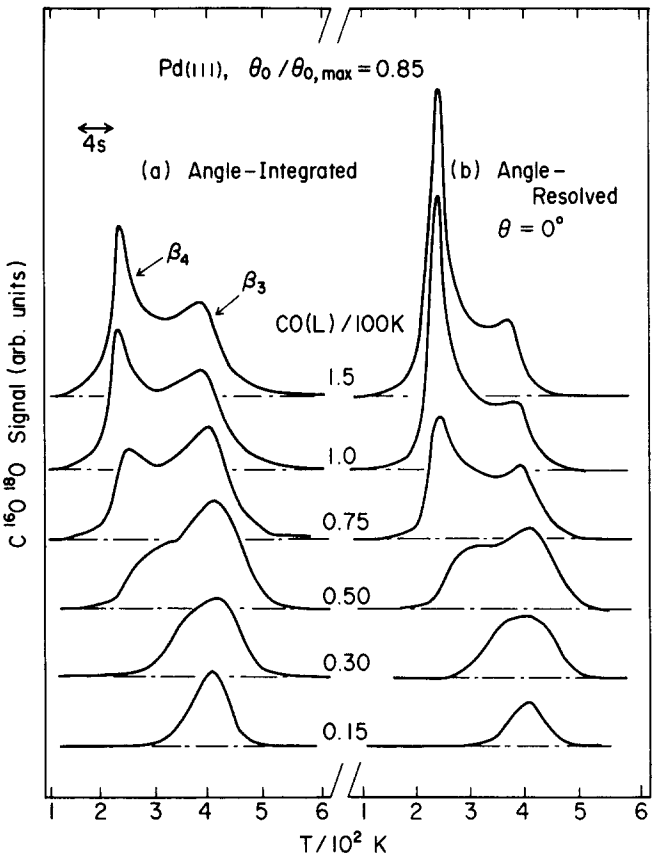

FIG. 9. CO_2 spectra generated at a high oxygen coverage and various CO exposures. The spectra were simultaneously recorded in both angle-integrated (a) and angle-resolved (b) forms.

Typical CO_2 spectra generated at different initial oxygen coverages observed in both forms were reproduced in Figs. 8 and 9. The surface was first exposed $^{18}O_2$ at 300 K. It was further exposed to $C^{16}O$ at 1.0×10^{-8} Torr in various amounts at 100 K and heated, while the amount of $C^{16}O^{18}O$ was simultaneously monitored with both mass spectrometers. The desorption angle was set at $\theta = 0°$ (θ is the angle between the surface normal and the collimator axis). Neither $C^{16}O_2$ nor $C^{18}O_2$ was observed. The usage of $^{18}O_2$ improved the ratio of the signal to noise of the mass spectrometer in the analyzer chamber. Oxygen 18 is frequently designated simply as O in the following. The sensitivity of the mass spectrometer was fixed during a series of experiments. No comparison is possible with the absolute intensity in different figures.

The ratio of β_4-CO_2 to β_1-CO_2 in the angle-integrated form is less than that in the angle-resolved form as seen in Fig. 8. It means that the desorption of β_4-CO_2 is directed more sharply towards the surface normal. This comparison became clear when the initial oxygen coverage was increased. When the coverage $\theta_O/\theta_{O,max} = 0.85$ (Fig. 9), the peak height ratio of β_4-CO_2 to β_3-CO_2 in the angle-integrated form was about 2 at 1.5 L CO. On the other hand a similar ratio became 5 at the normal direction in the angle-resolved form. The angular distribution of β_4-CO_2 is sharper than that of β_3-CO_2.

No new features were found in the desorption of CO and oxygen from coadsorption layers. Both desorptions of unreacted species occurred at temperatures higher than the CO_2 formation. When the CO exposure was 0.3 L in Fig. 9, no desorption of CO was found. Most of CO(a) was removed as CO_2. The desorption of O_2 decreased with an increase in the CO exposure. Above 0.6 L CO, the desorption of O_2 was hardly detected. The total amount of CO_2 formation became almost constant above 1 L CO.

The higher temperature CO_2 peak appeared at 410 K or below even with small CO exposures, when $\theta_O/\theta_{O,max} = 0.85$. This CO_2 involves mostly β_3-CO_2, since 0.15 L CO is already more than $Q_{CO,1}$. On the other hand CO_2 at 0.30 L CO or below and at $\theta_O/\theta_{O,max} = 0.13$ contains β_1-CO_2. Here the difficulty is found in the determination of the individual angular distribution of β_3- and β_1-CO_2 at small CO exposures. The kinetic behavior of β_3-CO_2 was analyzed when the surface covered largely with oxygen was exposed to CO in large amounts. Kinetic information of β_1-CO_2 was obtained, when CO was first dosed and then O_2 was introduced. In this adsorption sequence, O_2 can adsorb outside the CO domains. The superposition of $(\sqrt{3}\times\sqrt{3})R\,30°$ and $p(2\times2)$-O was observed. A series of β_1-CO_2 formation spectra is reproduced in Fig. 10. At small θ_{CO}, CO_2 peaked at 430 K. The peak was shifted to a somewhat higher temperature (445 K) with the increasing CO exposure. Above $\theta_{CO} = 0.1$, the peak shifted again to lower temperatures (350 K). Such behavior of CO_2 formation in this adsorption

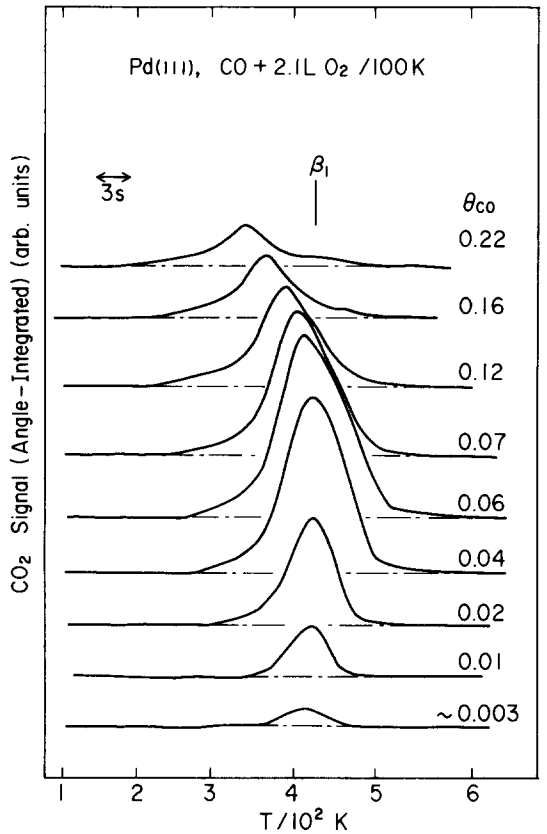

FIG. 10. Variation of β_1-CO_2 spectra with CO coverage. The surface was first exposed to CO and further to oxygen at 100 K.

sequence has previously been reported on Pd(111)[13] and also on Rh(111).[7]

The activation energy of CO_2 formation was estimated by using an isostere method.[16] A representative set of reaction isosteres is shown in Fig. 11. The logarithm of the peak maximum R_m was plotted against the reciprocal of the peak temperature T_m. The slope yielded 40 ± 10 kcal/mol as the activation energy for β_1-CO_2 formation. The activation energies for β_3- and β_4-CO_2 formation were also determined in the same way to be 30 ± 10 and 23 ± 7 kcal/mol, respectively. This method produced large errors, since the peak temperature was not shifted considerably by using heating rates in the range of 3–30 K/s. However this method alone is applicable in the present experiments, because the reaction orders with respect to CO and oxygen are not considered to be constant over a range of the coverage studied.

E. Angular distribution

Typical CO_2 formation spectra observed at various desorption angles are shown in Figs. 12 and 13. The angle-integrated spectra recorded simultaneously are also reproduced for comparison. The surface was first exposed to $^{18}O_2$ at 100 K, and annealed up to 250 K to remove oxygen admolecules and to produce a surface covered by $p(2\times2)$-O. At this stage the coverage of oxygen adatoms was $\theta_O/\theta_{O,max} = 0.80$. The surface was further exposed to $C^{16}O$ at 100 K and heated resistively. The amount of β_4-CO_2 was less than that of β_3-CO_2 when the CO exposure was 0.8 L, as seen in the angle-integrated form in Fig. 12. In the normal direction, the peak height of β_4-CO_2 was higher than that of β_3-CO_2. On the other hand, the former was less than the latter at large desorption angles. In other words, the peak of β_4-CO_2 decreased more rapidly than β_3-CO_2 with the increasing desorption angle. The peak temperature of the angle-resolved spectra remained invariant. The formation of β_4-CO_2 became predominant when the CO exposure was large (Fig. 13). The peak of β_4-CO_2 at the normal direction was much

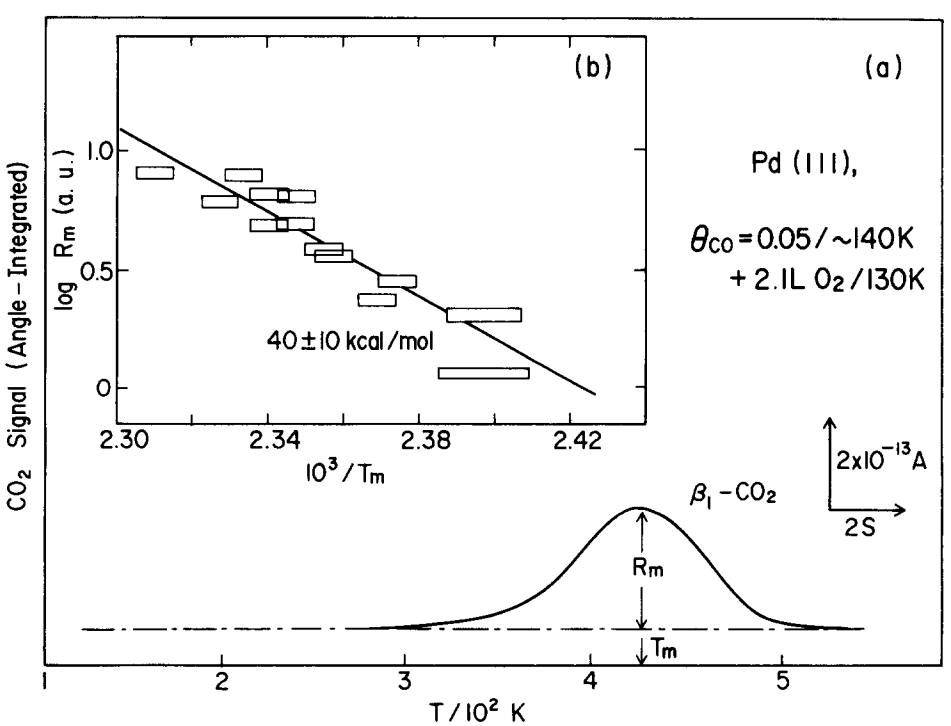

FIG. 11. A typical β_1-CO_2 spectrum (a) and the reaction isosteres (b). The surface covered with CO was exposed to oxygen at 130 K. The heating rate was varied from 3 to 30 K/s.

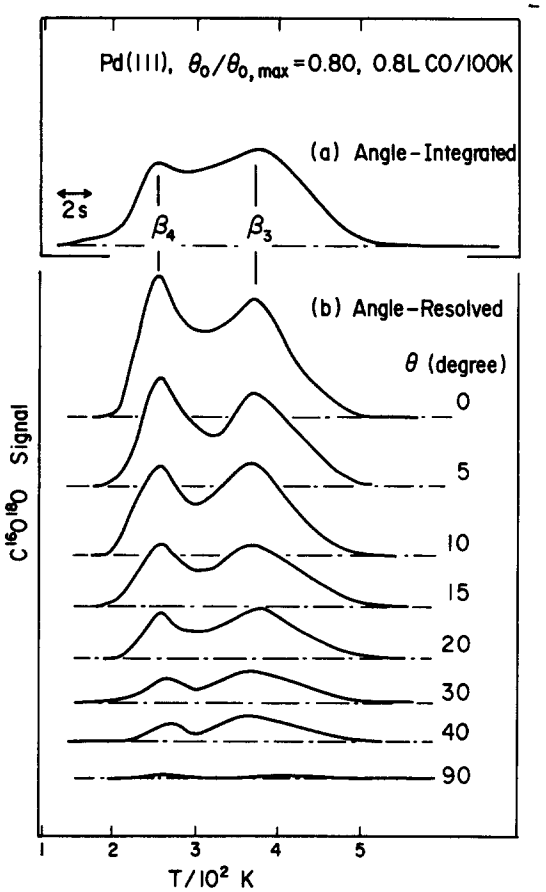

FIG. 12. (a) CO_2 formation spectrum in the angle-integrated form at a medium CO exposure. (b) Angle-resolved CO_2 spectra observed at various desorption angles.

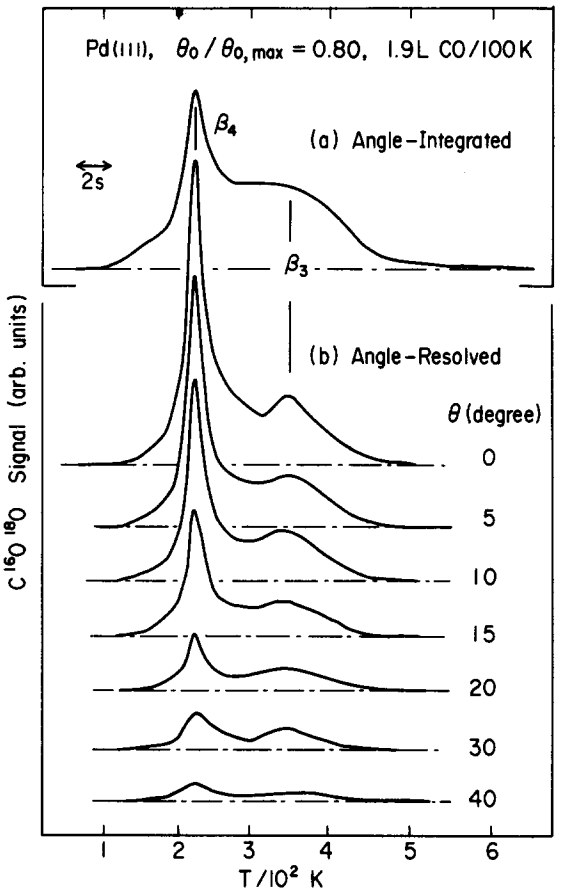

FIG. 13. (a) CO_2 formation spectrum in the angle-integrated form at a high CO exposure. (b) Angle-resolved CO_2 spectra observed at various desorption angles.

higher than that of β_3-CO_2. It decreased rapidly with the increasing desorption angle. It became comparable with that of β_3-CO_2 at large desorption angles.

The relative peak height was plotted against the desorption angle in Figs. 14 and 15. The peak height was corrected by considering that an increasing area of the front face of the crystal falls inside the solid angle of acceptance of the apertures of the collimator, when the crystal is rotated away from the surface normal. Experimental data for β_3-CO_2 were scattered. The angular distribution was summarized in the usage of power series of $\cos\theta$. The peak signal varied as $(\cos\theta)^d$ with $d = 15$–25 except for the case of 0.4 L CO. The latter showed $d = \sim 12$. This CO_2 contained β_1-CO_2, which shows a broader distribution.

β_4-CO_2 showed the sharpest angular distribution as shown in Fig. 15. It yields $d = 30$–40 below $\theta = 15°$. Data above $\theta = 15°$ indicate a broader distribution, i.e., $d = \sim 20$. The angular distribution did not depend on the coverage of CO. The CO exposure changed the amount of β_4-CO_2. This means that the exposure changed the extension of regions with (2×1) periodicity. The angular distribution is affected by the local structure around the reaction site.

The angular distribution of β_1-CO_2 is shown in Fig. 16. In this case the surface was first exposed to CO in small amounts at 100 K and further to $^{18}O_2$ in large amounts. The angular distribution showed $d = 4$–8. This is quite similar to the angular distribution of β_1-CO_2 produced on Rh(111).[7]

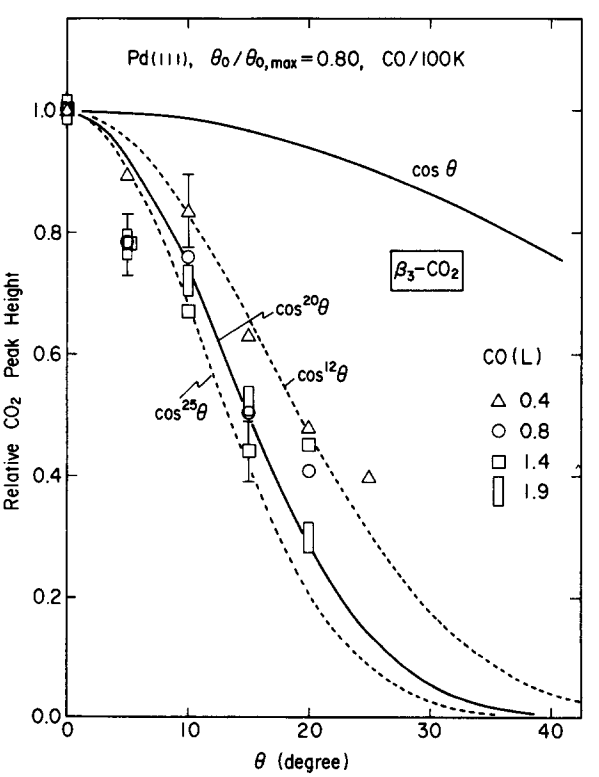

FIG. 14. Angular distribution of the desorption of β_3-CO_2. The surface covered with oxygen was exposed to CO at 100 K. The heating rate was ~ 22 K/s.

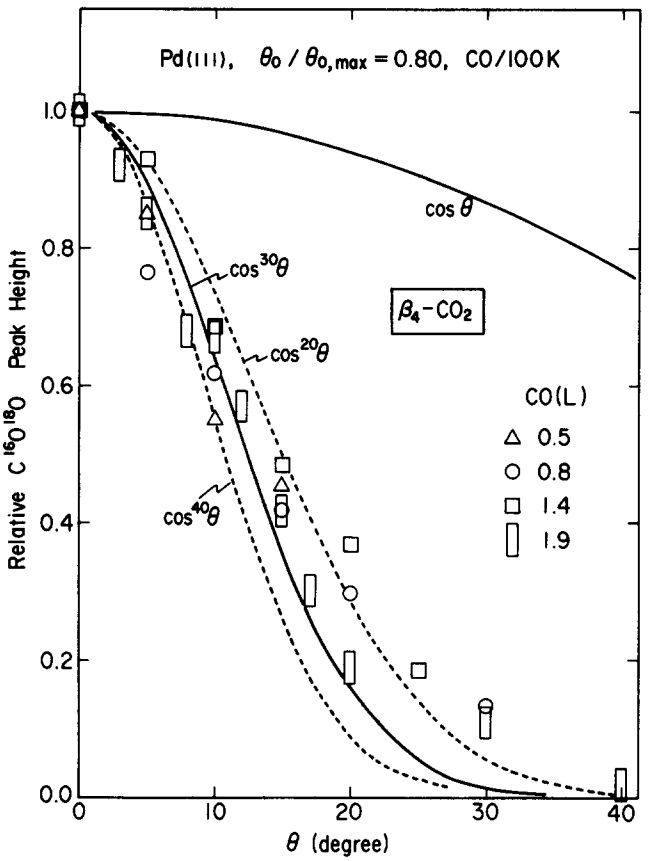

FIG. 15. Angular distribution of the desorption of β_4-CO_2. The surface covered by oxygen was exposed to CO at 100 K and heated at a rate of 22 K/s.

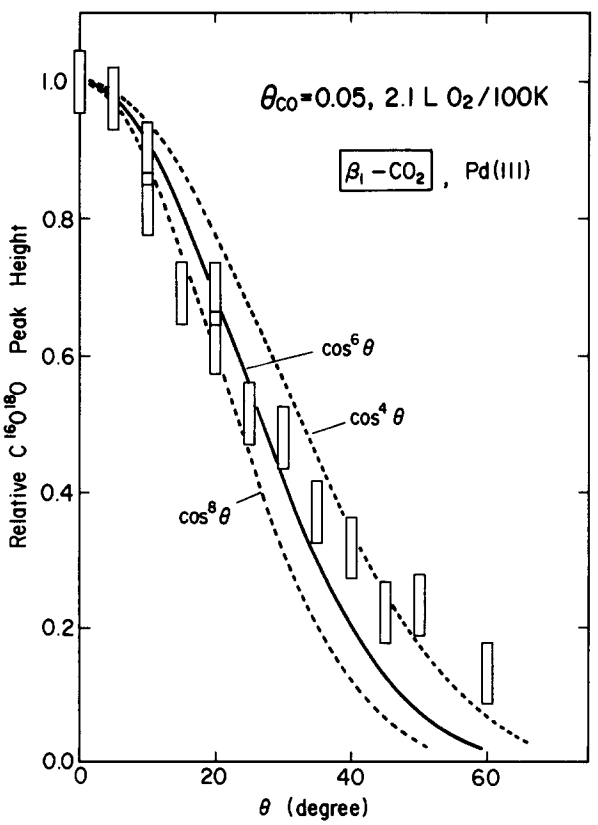

FIG. 16. Angular distribution of β_1-CO_2. The surface was first exposed to CO and further to O_2 at 100 K. The heating rate was 20 K/s.

Engel and Ertl reported a cosine distribution of the desorption of CO_2 produced on Pd(111) at a steady state at 570 K and under low reactant pressure.[17] Their results refer to very low coverage, but the reason for this disagreement is not clear at present.

IV. DISCUSSION

In this section we will discuss several factors which contribute to the angular distribution.

The desorption of CO_2 from the physisorption state shows a simple cosine distribution.[3,4] In this case, no excess translational energy is expected as compared with the surface temperature.[18] On the other hand, the sharp angular distribution of the reaction product indicates that the molecules leave the surface with an excess translational energy. The origin of such an excess translational energy of desorbing molecules has typically been explained by a simple one-dimensional model proposed by Comsa[19] and Willigen.[20] In this model the angular distribution is related to the activation barrier perpendicular to the surface for the *adsorption*. Recent work by Comsa's group[10] recognizes the importance of this model in the case of H_2 desorption.

A potential energy diagram illustrating the CO_2 formation is shown in Fig. 17. The initial state of the reaction consists of CO(a) and O(a). The initial adsorption energy of CO and oxygen is 34[21] and about 55[22] kcal/mol, respectively. The heat of the reaction, $CO(g) + 1/2\,O_2(g) \rightarrow CO_2(g)$, is -67.5 kcal/mol.[23] The potential energy of the initial state was estimated to be 9 kcal/mol above the gaseous CO_2. The activation energy of β_1-CO_2 formation is 40 ± 10 kcal/mol. Hence the activated state is about 50 kcal/mol above the

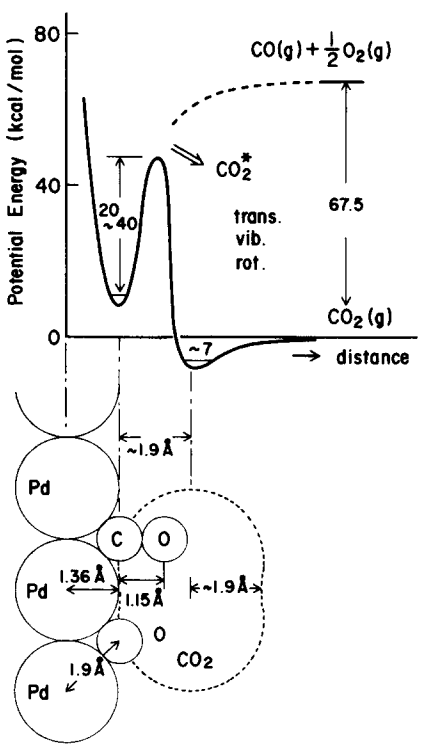

FIG. 17. Potential energy diagram for CO_2 formation.

gaseous level. The translational energy of β_1-CO_2 desorbed at the normal direction was estimated to be only about 4 kcal/mol, by using Doyen's equation.[24] A similar value was obtained with Willigen's equation.[14] The activation energy of the reaction is not transferred effectively into the translational mode. The initial state for the formation of β_3- and β_4-CO_2 may be raised, since the heat of adsorption of the reactants must be decreased by the increasing repulsive interaction in the dense coadlayers. The activated state, however, may not be raised significantly, because the activation energy is also decreased considerably. The translational energy at the normal direction of β_3- and β_4-CO_2 was estimated in the same way as described above to be 9.2 and 7.3 kcal/mol, respectively. Only a small portion of the activation energy is transferred into the translational mode.

The activation energy for the reaction involves several contributions, i.e., the breakaway of the adsorption bonds of the reactants, the approach of the reactants, the relaxation of the surface atom arrangements, the evacuation of a space for the product molecule, and so on. There is a small possibility that the first three factors contribute to the velocity or the angular distribution. For example, the reactants must approach each other to yield CO_2, although the interaction between CO(a) and O(a) is repulsive.[13] They are compelled to overwhelm the repulsive force. This interaction energy may be stored in the internal mode, however it is not expected to be transferred into the translational mode. Because the angular distribution is controlled by the interaction between the whole nascent CO_2 molecule and the surface. The fourth factor plays a major role in determining the angular distribution. This factor will be discussed in the following two paragraphs.

Gaseous CO_2 molecules can be adsorbed in the physisorption state. The desorption from this state is complete below 130 K.[2–5] The adsorption energy is close to the heat of sublimation of solid carbon dioxide, 6.0 kcal/mol.[23] The latter is a typical molecular crystal, in which the interaction between neighboring molecules is due to dispersion forces. These forces may play a major role in the physisorption bond. The equilibrium position was estimated to be about 3.3 Å from the surface plane (the center of surface Pd atoms) from van der Waals' radius.[25] The position of CO_2 formation must be closer to the surface than this physisorption site. The reactants CO(a) and O(a) are chemisorbed and their equilibrium positions are much closer to the surface plane. CO is chemisorbed in a bridged site on Pd(111).[26] The position of

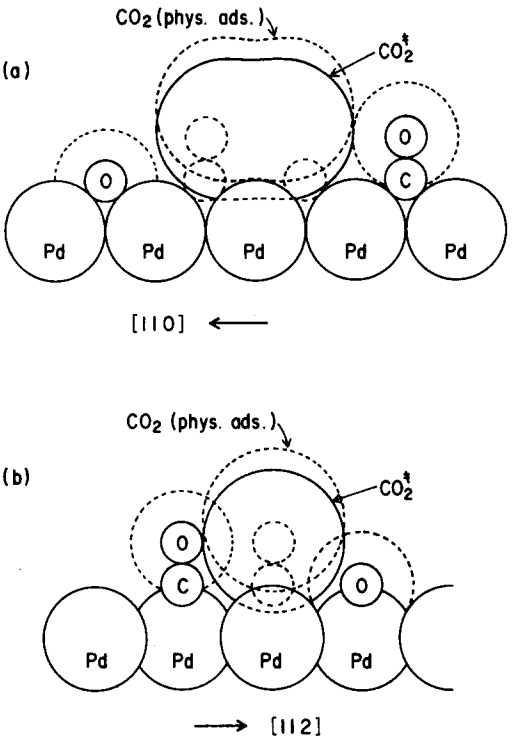

FIG. 18. Sketches of sections of the reaction site for β_4-CO_2. (a) [110] direction; (b) [112] direction. Dotted curves are drawn by using van der Waals' radii. Double dagger indicates a position of the activated state (see the text).

carbon is about 1.4 Å from the surface.[27] Oxygen adatoms may be located at almost the same distance. The size of an oxygen adatom and also of a Pd atom is drawn by referring to Pauling's covalent radii.[28] The position of carbon of CO(a) is about 1.9 Å closer to the surface than that of CO_2 physisorbed. Even if the position of carbon in the activated state is located at the center of both carbon atoms, it is still about 1 Å closer to the surface than that of CO_2 physisorbed. This consideration suggests strongly that CO_2 molecules produced receive a significant repulsive force from the surface the very instant that they are produced, or during the formation. This repulsive force can increase the velocity of the product CO_2 along the surface normal.

In order to discuss the angular distribution of desorbing molecules, we should consider the motion parallel to the surface plane, as well as to the surface normal. In Willingen's model no restriction is introduced in the motion along the

TABLE II. Angular distribution of CO_2 produced on different surface planes. It is represented as $(\cos\theta)^d$.

CO_2	Reaction site	Pd(111)	Rh(111)	Pt(111)
β_1	Between (2×2)–O and $(\sqrt{3}\times\sqrt{3})R$ 30°–CO domain	$d=6\pm2$	$d=4\pm1$	$d=9\pm2$
β_2	In (2×2)–O domain	...	15 ± 3	...
β_3	Between $(\sqrt{3}\times\sqrt{3})R$ 30°–O and $(\sqrt{3}\times\sqrt{3})R$ 30°–CO domain	20 ± 5	...	...
β_4	In (2×1)–(CO–O) domain	30 ± 10	...	...
	Reference	Present work	7	3

surface. The motion of desorbing CO_2 may be restricted parallel to the surface plane, by collision with the surrounding CO and oxygen adatoms, when the reaction site is closely surrounded by unreacted adspecies. This may result in the collimation of the desorbing CO_2 along the surface normal. This interaction may be discussed by considering that their size is described by van der Waals' radii, because no chemical bond between CO_2 and CO(a) or O(a) can be considered. Figure 1 shows the size of a CO_2 molecule estimated from van der Waals' radii. The lateral extension of CO(a) and O(a) is roughly described by the radius of oxygen, i.e., 1.40 Å.[28] Now we can draw sections of the adsorption structures. The upper panel in Fig. 18 shows a section of the reaction site for β_4-CO_2 along with the [110] direction. The activated complex is assumed to be at the center of both carbon atoms in CO(a) and CO_2(a). CO_2 is in close contact with CO(a) and O(a). In the [112] direction, the electron clouds of producing CO_2 are already overlapped with those of surrounding CO and oxygen adatoms. It means that CO_2 molecules will receive a strong repulsive force from the coadsorbates parallel to the surface. Such restriction in the motion by adsorbates is not expected in the case of β_1-CO_2, since there is a significant free space around sites for the CO_2 formation. This collimation effect may play a role in determining the angular distribution of β_3-CO_2.

In Table II are listed the power of cosine θ in the expression of the angular distribution of the CO_2 desorption reported so far. Two different reaction sites were observed on Rh (111).[7] One is between separate domains of CO and (2×2)–O domains. This CO_2 peaks around 450 K. The other is inside (2×2) oxygen domains. The oxygen lattice is not compressed over Rh(111). CO can adsorb in this lattice. The interaction of CO with oxygen inside the domains produces β_2-CO_2. It peaks around 400 K. The angular distribution of the former indicates $d = 4 \pm 1$, and the latter $d = 15 \pm 3$. Over Pt(111) only a single CO_2 peak was observed around 300 K, irrespective of the coverages of CO and oxygen adatoms. Separate domains of oxygen and CO were observed.[29] This CO is assigned to β_1-CO_2.

Now we find that the more closely the reaction site is surrounded, the sharper the angular distribution is. These results strongly suggest that the motion of desorbing CO_2 is restricted in parallel to the surface plane. The collimation effect is not expected to increase the velocity of desorbing CO_2, although it may sharpen the angular distribution. It will be further tested when the detail of the energy distribution among the various degrees of freedom can be analyzed as a function of the desorption angle. The above consideration predicts that the angular distributions of β_4-CO_2 would depend on the crystal azimuth.

[1](a) T. Engel and G. Ertl, Adv. Catal. **28**, 1 (1979); (b) T. Engel, *The Chemical Physics of Surfaces and Heterogeneous Catalysis*, edited by P. Woodruff and D. A. King (Elsevier, Amsterdam, 1982), Vol. 4, p. 73; (c) G. Ertl, Catal. Sci. Technol. **4**, 209 (1983); (d) G. Ertl, *Chemistry and Physics of Solid Surfaces*, edited by R. Vanselow and W. England (Chemical Rubber, Boca Raton, FL, 1983), Vol. 3, p. 19.

[2]P. R. Norton, Surf. Sci. **44**, 624 (1974); P. R. Norton and P. J. Richards, *ibid.* **49**, 567 (1975).

[3]T. Matsushima, Surf. Sci. **127**, 403 (1983).

[4]T. Matsushima, J. Catal. **83**, 446 (1983).

[5]R. L. Palmer and J. N. Smith, Jr., J. Chem. Phys. **60**, 1453 (1974).

[6](a) C. T. Campbell, G. Ertl, H. Kuipers, and J. Segner, J. Chem. Phys. **73**, 5862 (1980); (b) J. Segner, C. T. Campbell, G. Doyen, and G. Ertl, Surf. Sci. **138**, 505 (1984).

[7]T. Matsushima, T. Matsui, and M. Hashimoto, J. Chem. Phys. **81**, 5151 (1984).

[8]T. Matsushima, J. Phys. Chem. **88**, 202 (1984).

[9]C. A. Becker, J. P. Cowin, L. Wharton, and D. J. Auerbach, J. Chem. Phys. **67**, 3394 (1977).

[10]G. Comsa, *Proceedings of the International School on Material Science and Technology, Dynamics of Gas Surface Interactions*, edited by G. Benedek and V. Valbusa (Springer, Erice, 1982), p. 117.

[11](a) D. A. Mantell, S. E. Ryali, B. L. Halpern, G. L. Haller, and J. B. Fenn, Chem. Phys. Lett. **81**, 185 (1981); D. A. Mantell, S. E. Ryali, and C. L. Haller, *ibid.* **102**, 39 (1983); D. A. Mantell, K. Kunimori, S. E. Ryali, G. L. Haller, and J. B. Fenn, J. Vac. Sci. Technol. A **3**, 1663 (1985).

[12]S. L. Bernasek and S. R. Leone, Chem. Phys. Lett. **84**, 401 (1981).

[13]H. Conrad, G. Ertl, and J. Küppers, Surf. Sci. Sci. **76**, 323 (1978).

[14]T. Engel, J. Chem. Phys. **69**, 373 (1978).

[15]T. Matsushima, Surf. Sci. **157**, 297 (1985).

[16]J. Falconer and R. J. Madix, J. Catal. **48**, 262 (1977).

[17]T. Engel and G. Ertl, J. Chem. Phys. **69**, 1267 (1978).

[18]J. E. Hurst, C. A. Becker, J. P. Cowin, K. C. Janda, L. Wharton, and D. J. Auerbach, Phys. Rev. Lett. **43**, 1175 (1979).

[19]G. Cosma, J. Chem. Phys. **48**, 3235 (1968).

[20]W. van Willigen, Phys. Lett. A **28**, 80 (1968).

[21]H. Conrad, G. Ertl, J. Koch, and E. E. Latta, Surf. Sci. **43**, 462 (1974); G. Ertl and J. Koch, Z. Naturforsch. Teil A **25**, 1906 (1970).

[22]H. Conrad, G. Ertl, J. Küppers, and E. E. Latta, Surf. Sci. **65**, 245 (1977).

[23]*Lange's Handbook of Chemistry, 20th*, edited by J. A. Dean (McGraw-Hill, New York, 1979).

[24]G. Doyen, Vacuum **32**, 91 (1982).

[25]T. Kihara and A. Koide, Adv. Chem. Phys. **33**, 51 (1975).

[26]F. M. Hoffmann, Surf. Sci. Rep. **3**, 107 (1983).

[27]R. J. Behm, K. Christmann, G. Ertl, and M. A. van Hove, J. Chem. Phys. **73**, 2984 (1980).

[28]L. Pauling, *The Chemical Bond* (Cornell University, New York, 1967).

[29]J. L. Gland and E. B. Kollin, J. Chem. Phys. **78**, 963 (1983).